Heliyon 9 (2023) e18424

Contents lists available at ScienceDirect

Heliyon

journal homepage: www.cell.com/heliyon

Analysis of urban heat islands with landsat satellite images and GIS in Kuala Lumpur Metropolitan City

Nasrin Adlin Syahirah Kasniza Jumari [a], Ali Najah Ahmed [b,h,**], Yuk Feng Huang [a,*], Jing Lin Ng [c], Chai Hoon Koo [a], Kai Lun Chong [d], Mohsen Sherif [e,f], Ahmed Elshafie [g]

[a] *Department of Civil Engineering, Lee Kong Chian Faculty of Engineering and Science, Universiti Tunku Abdul Rahman, Jalan Sg. Long, Bandar Sg. Long, 43000, Kajang, Selangor, Malaysia*
[b] *Department of Civil Engineering, College of Engineering, Universiti Tenaga Nasional, Kajang, 43000, Selangor, Malaysia*
[c] *School of Civil Engineering, College of Engineering, Universiti Teknologi Mara (UiTM), 40450 Shah Alam, Selangor, Malaysia*
[d] *Faculty of Engineering & Quantity Surveying, INTI International University (INTI-IU), Persiaran Perdana BBN, Putra Nilai, Nilai, 71800, Negeri Sembilan, Malaysia*
[e] *National Water and Energy Center, United Arab Emirates University, Al Ain P.O. Box 15551, United Arab Emirates*
[f] *Civil and Environmental Eng. Dept., College of Engineering, United Arab Emirates University, Al Ain, 15551, United Arab Emirates*
[g] *Department of Civil Engineering, Faculty of Engineering, University of Malaya (UM), 50603, Kuala Lumpur, Malaysia*
[h] *Institute of Energy Infrastructure (IEI) , Universiti Tenaga Nasional (UNITEN), 43000, Selangor, Malaysia*

A R T I C L E I N F O

Keywords:
Urban heat island
Land surface temperature
GIS software
Landsat images

A B S T R A C T

Cities are growing geographically in response to the enormous increase in urban population; consequently, comprehending growth and environmental changes is critical for long-term planning. Urbanization transforms naturally permeable surfaces into impermeable surfaces, causing an increase in urban land surface temperature, leading to the phenomenon known as urban heat islands. The urban heat islands are noticeable across Malaysia's rural communities and villages, particularly in Kuala Lumpur. These effects must be addressed to slow, if not halt, climate change and meet the Paris Agreement's 2030 goal. The study posits an application of thermal remote sensing utilizing a space-borne satellite-based technique to demonstrate urban evolution for urban heat island analysis and its relationship to land surface temperature. The urban heat island (UHI) was analyzed by converting infrared radiation into visible thermal images utilizing thermal imaging from remote sensing techniques. The heat island is validated by reference to the characteristics of the normalized difference vegetation index (NDVI), which define the land surface temperature (LST) of distinct locations. Based on the digital information from the satellite, the highest temperature difference between urban and rural regions for a few chosen cities in 2013 varied from 10.8 to 25.5 °C, while in 2021, it ranged from 16.1 to 26.73 °C, highlighting crucial temperature changes. The results from ANOVA test has substantially strengthened the credibility of the significant temperature changes. Some notable reveals are as follows: The Sungai Batu area, due to its rapid development and industry growth, was more vulnerable to elevated urban heat due to reduced vegetation cover; therefore, higher relative vulnerability. Contrary, the Bukit Ketumbar area, which region lies in the woodland region, experienced the lowest, with urban heat islands reading from 2013 at −0.3044 and 0.0154 in 2021. It shows that despite having urban heat islands increase two-fold from 2013 to 2021, increasing the amount of vegetation

* Corresponding author.
** Corresponding author.
E-mail addresses: mahfoodh@uniten.edu.my (A.N. Ahmed), huangyf@utar.edu.my (Y.F. Huang).

https://doi.org/10.1016/j.heliyon.2023.e18424
Received 30 January 2023; Received in revised form 17 July 2023; Accepted 17 July 2023
Available online 22 July 2023

coverage is a simple and effective way of reducing the urban heat island effect, as evidenced by the low urban heat islands in the Bukit Ketumbar woodland region. The study findings are critical for advising municipal officials and urban planners to decrease urban heat islands by investing in open green spaces.

1. Introduction

1.1. Background

Long-term variations in temperature and weather are some components that make up climate change [1]. Changes in land use and land cover (also known as LULC) may affect ecosystems at all levels, from the local front to the global entity, contributing to the climate change phenonmenon. Although the La Nina climate pattern in the tropical Pacific had cooled the planet in 2021, the NOAA National Centre for Environmental Information's 2021 Global Climate Report revealed that in every month of 2021, temperatures were above-average [2]. A natural phenomenon known as an urban heat island, or UHI for short, is one of the most important factors contributing to climate change. The phenomenon known as an urban heat island, is prevalent in numerous places throughout the world [3,4]. An urban heat island is a city or area with considerably higher temperatures than the surrounding areas. Another interpretation of an urban heat island is that of a city with greater urban air temperatures than the surrounding rural areas. It comes about primarily due to the high thermal capacity of building materials; a decrease in latent heat flow due to increased surface water drainage; an increase in anthropogenic heat, and tandem with a reduction in the quantity of open and green space in urban contexts [5]. It occurs when large concentrations of paved surfaces, buildings, and other heat-absorbing and holding surfaces replace the natural ground cover in metropolitan settings. As a result, the temperature rises, increasing energy expenditures, contributing to an increase in heat-related disease and death, and contributing to increased air pollution [6]. Man-made structures, such as homes and roads, absorb and re-emit solar heat more efficiently than natural habitats, such as forests and bodies of water. Because of the high density of these structures and the scarcity of greenery close by, the urban areas produce "islands" with higher temperatures in comparison to the surrounding more rural locations [7]. Also, the variation of LST throughout the day and night time also affects the UHI. According to research conducted by Bala, Prasad [8], the daytime was mostly influenced by vegetation, while the nighttime was influenced by the imperviousness of the surface cover. Another research by Bala et al.,Bala, Prasad [9] found a positive correlation between the barren ground and built-up areas, with the daytime UHI, a reverse effect of that by vegetation cover.

Kuala Lumpur City is the capital of Malaysia and is considered the most populous metropolitan district in the country. It has an estimated population of 8,420,000 people. The living culture in Kuala Lumpur invariably requires automobile rides to get around, air conditioners to stay comfortable, continual building development, and continuous power generated in a large number of Kuala Lumpur skyscrapers. These lifestyles are but a few of the reasons for the rising temperatures in Kuala Lumpur [10,11]. Overexposure to heat has been linked to decreased job productivity, household spending patterns, and overall living standards. It is made worse by the UHI, and in megacities, this typically goes anywhere between 0.1 and 3° Celsius. According to an article in The Star News on July 5th, the UHI readings in Kuala Lumpur are in the range of 4–6° Celsius, often reaching their highest point during the night-time hours, affecting the repercussions for both human health and productivity of labour. The UHI effect contributes to haze pollution events, which have severe economic consequences. For instance, it was estimated that the damage caused by the haze in Kuala Lumpur in 1997 was RM1.41 billion [12].

In Malaysia, and particularly in Kuala Lumpur, significant research has been done to investigate urban heating. Due to continual urbanization, Kuala Lumpur is experiencing a worsening crisis concerning the overheating of its metropolitan areas. Previous studies have emphasized the global-scale analysis of Malaysia, where the chosen study area was Greater Kuala Lumpur which is considered the boundary of Metropolitan Kuala Lumpur in Malaysia. Research focusing on one of the towns, Kuala Lumpur, was rarely reported. Sham Sani initiated his investigation in the early 1970s, and throughout the next two decades, he observed the escalation of urban heating [5]. In addition, Morris, Chan [13] used the numerical model to study the historical local urban climate changes that occurred throughout a decade, from the year 1999–2011, of urbanization. To the best of the authors' knowledge, Greater Kuala Lumpur was the focus of most research in the literature review, rather than the city of Kuala Lumpur, which is frequently ignored. With the help of QGIS and ArcGIS to model the urban climatic features of Kuala Lumpur, the effect of the urban heat island on Kuala Lumpur can be modelled and studied.

1.2. Literature review

Methodologies of the UHI Analysis by Mahdavi, Kiesel [14] served as the basis for a study of UHI in central European cities. They have presented the findings of a study financed by the EU on Urban Heat Islands (UHI) in Central European cities. Their research aims to examine the consequences of UHI and develop and evaluate mitigation and adaptation strategies. Short-term and long-term analyses of UHI were conducted, with the short-term duration being hourly and the long-term length being 30 years. Based on their modeling efforts, it can be concluded that the high domain complexity of urban microclimate modeling reduces model trustworthiness. Even sophisticated and theoretically coherent simulation systems might produce erroneous results when given insufficient input data. They investigated the significant relationships between urban characteristics (morphology, materials) and microclimatic parameters. Such correlations would provide efficient preliminary estimates of the effectiveness of mitigating strategies [14].

The UHI can be presented to the audience in a variety of ways. The study conducted by Acosta, Vahdatikhaki [15] proved the methods for simulating UHI at the street level. To summarise, the four steps offered were data collection, data preparation, model construction, and the creation of the UHI Assessment Matrix. During the data collection period, variables of socioeconomic situations and urban morphology are obtained from publicly accessible databases. The data preparation phase involves feature extraction from raw data. In the model development phase, decision trees and random forests are used to solve the problem of identifying the characteristics that best define UHI at the meso level. Specifically, this phase focuses on identifying the traits that best define UHI at the meso level. A tree regression technique is used to categorize streets based on temperature for the UHI Assessment Matrix to reduce the heat island impact. In addition, at this stage, users might choose to use machine learning instead of undertaking mapping analysis using modeling. Similarly, LST used the same phases as UHI.

As was said before, one of the ways to demonstrate and investigate UHI is through mapping analysis, which may be achieved with the use of GIS. Mutani, Todeschi [16] adopted several techniques for mitigating the effects of UHI in the Hiroshima region. In a prior study applicable to the Metropolitan City of Turin (Italy), the microclimate of outdoor places was analyzed by comparing the reported outdoor air temperatures. In the city of Hiroshima case study, they utilized the UHI models that they had built earlier. The goal was to develop a basic GIS-based model for simulating hourly air temperature using linear regression as the forecasting method.

Thermal bands in remote sensing satellites like Landsat are a system of U.S. satellites designed to collect and send information about the earth's natural resources, topography, etc. One of the Landsat used in the UHI mapping analysis is the Landsat 8. The LST can be calculated using the thermal bands of the Landsat TM, ETM+, and Landsat 8 satellite photography products [17]. Landsat 8 records numerous frequency ranges over the electromagnetic spectrum — a colour but not always perceptible to the human eye. Each range is known as a band, and the Landsat 8 possesses eleven. Landsat's red, green, and blue sensors are numbered 4, 3, and 2, respectively [18]. Another interesting study by Bala, Prasad [19] where they compared the disaggregated coarse-resolution MODIS using NDBI index with that of Landsat 8. They demonstrated that downscaling LST using MODIS-NDBI was preferable to utilizing Landsat 8.

With the QGIS, rasters provide a deeper understanding of the terrain they represent. The QGIS has 14 distinct raster analysis options. Grid (Moving average) is a straightforward algorithm for averaging data. It searches for values using an elliptical moving window and averages all data points within the window. Grid (Data metrics) computes particular data metrics using the specified window and output grid form. Aspect utilizes the compass direction a slope faces. The pixels will have an azimuth value between 0 and 360° measured from the north [20].

1.3. Problem statement

Global warming has influenced many lives in Malaysia, as has been so, in the majority of other nations, during the past several years. Rising temperature is the principal contributor to global warming, and this is influenced by the ever increasing number of buildings and skyscrapers, especially in the Kuala Lumpur area. Hence, one must conduct the LST and UHI analysis to help monitor Kuala Lumpur's temperature. The fundamental objective of research on UHI is to establish whether there has been a significant shift in the regularity of the land surface temperatures. To accurately decipher the changes, an analysis of the LST can be made using the Geographic Information System (GIS) software. GIS store, retrieve, analyze, and display geographic data using a database of spatial attributes [21]. A dependable analysis mapping could provide an initial imaging of the past LST and the UHI and give warnings to minimize the likelihood of drought in the urban area.

1.4. Objectives

The aims were first investigated utilizing GIS analytic tools to analyze the Land Surface Temperature (LST) in Kuala Lumpur from 2013 to 2021 using Landsat 8 image data. Second, the use GIS analytical techniques to compare the analysis and developments of LST and UHI between the years 2013 and 2021 in Kuala Lumpur was next carried out. Third, was to evaluate the assessment and changes of LST and UHI between the years 2013 and 2021. The experiment's findings might be used to provide extra research resources to mitigate the effects of rising LST and UHI.

2. Methodology

2.1. Case study area

Kuala Lumpur, the capital and largest city of Malaysia, was chosen as the site of this study. It is the most populous city in Malaysia and is regarded as one of the cities in Asia that is seeing the most rapid expansion. According to the census, the area being studied is 243 km^2 (94 sq mi) in size, and where 8,420,000 people live there—a growth of 2.55% from 2021. It is one of Southeast Asia's fastest-developing metropolitan areas in terms of economic and demographic development. Furthermore, it was the sixth most visited city in the world in 2019, making it one of the world's most prominent cities for tourism and retail shopping. This city is home to three of the ten largest retail malls around the entire globe.

31- point locations were used across the capital to observe the UHI values. These Kuala Lumpur locales have a high population density and construction areas. For instance, the Kuala Lumpur parliamentary constituency of Wangsa Maju has the highest population density in the country, with 13,475 persons per square kilometer. The Persiaran KLCC area consists of numerous skyscrapers and buildings that contribute to the high UHI intensity of Kuala Lumpur. Another area, Bangsar, is the go-to area for its distinctive cafe buildings and art museum. The capital city is Kuala Lumpur, which is depicted in Fig. 1 as having a significant number of higher

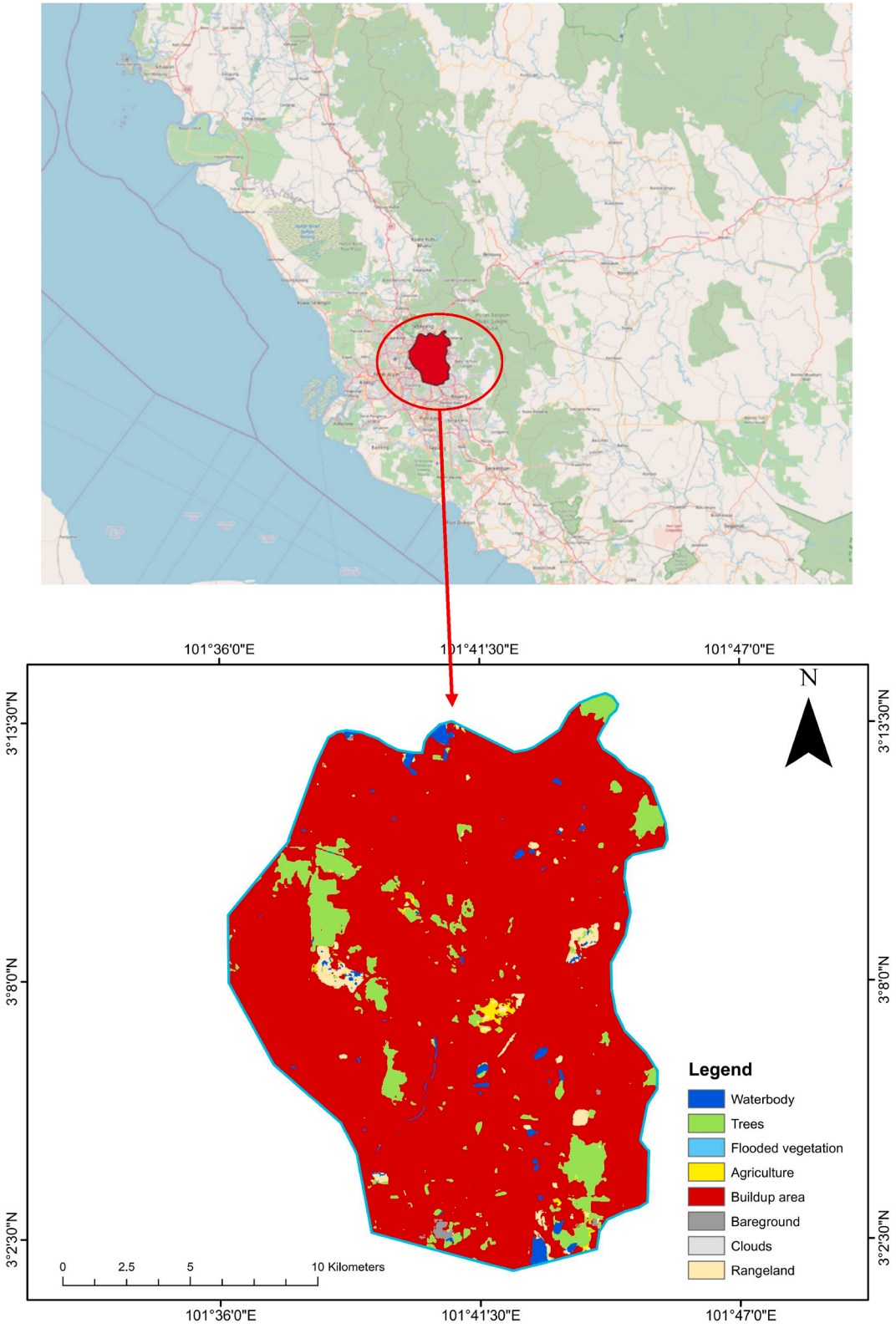

Fig. 1. Point locations in KL.

education institutions, elementary and secondary schools, etc.

The rural area reference used in this paper is Pulau Tengah, Selangor. Located at the mouth of the Klang River delta in the state of Selangor, there lies a deserted island known as Pulau Tengah. It is a mangrove swamp that covers the area. Fig. 2 shows the reference point coordinates at 2.9797 latitudes and 101.2257 longitudes. Fig. 3 depicts the flowchart of the study method.

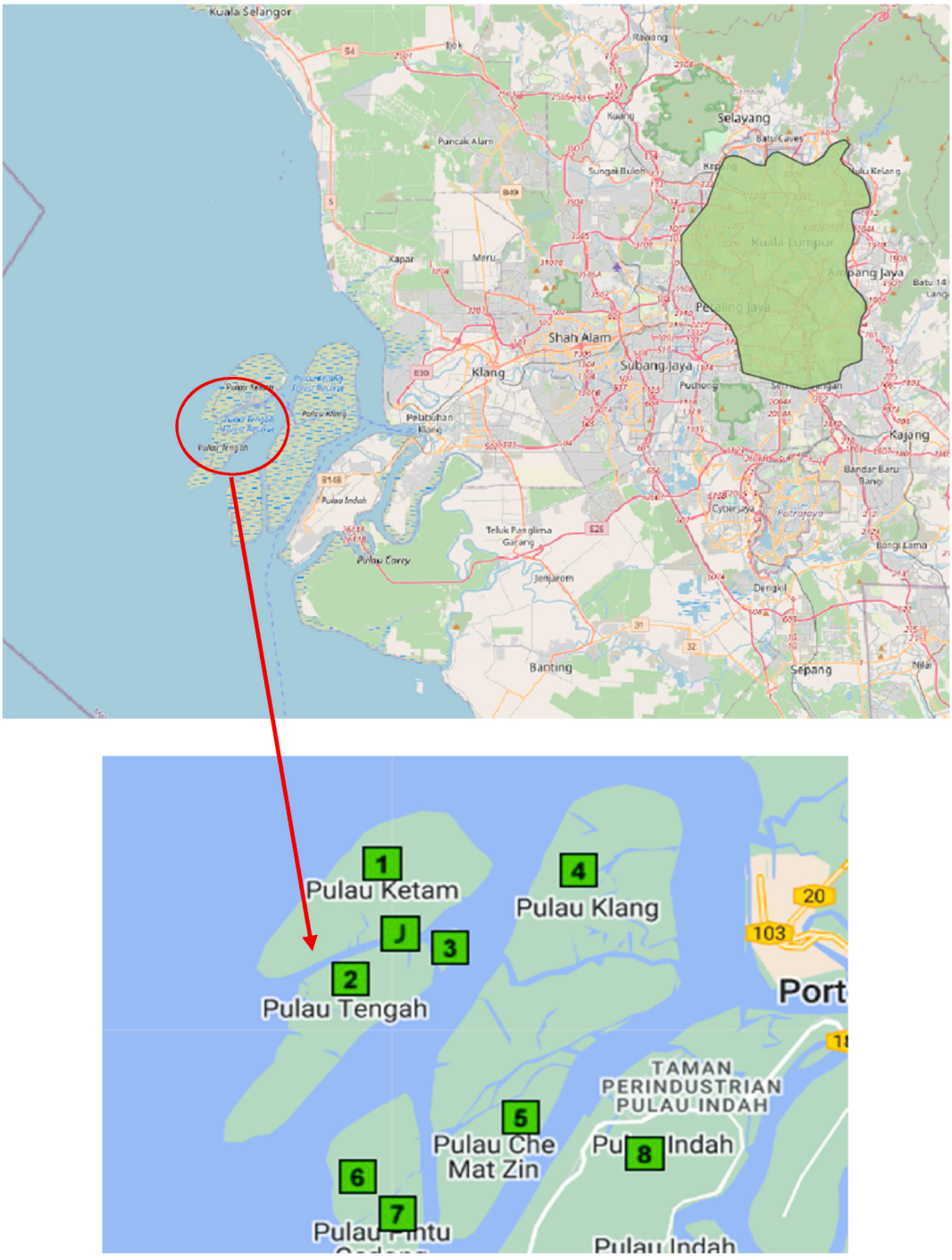

Fig. 2. Location of Pulau Tengah.

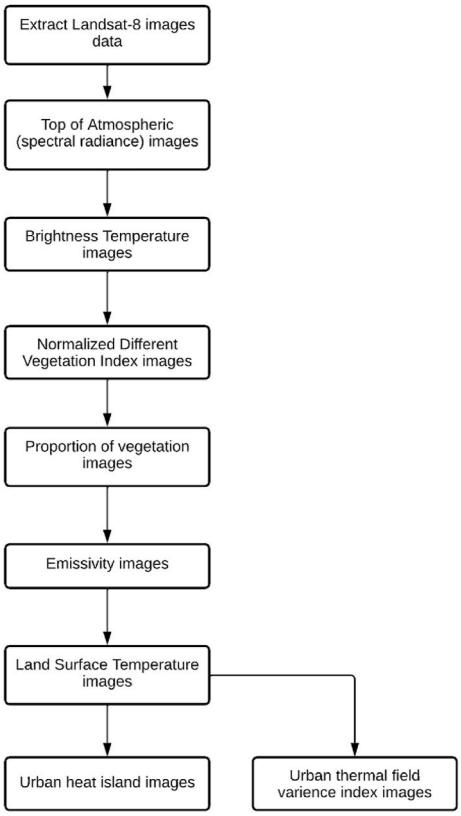

Fig. 3. Flowchart diagram to obtain the UHI and UTFVI mapping.

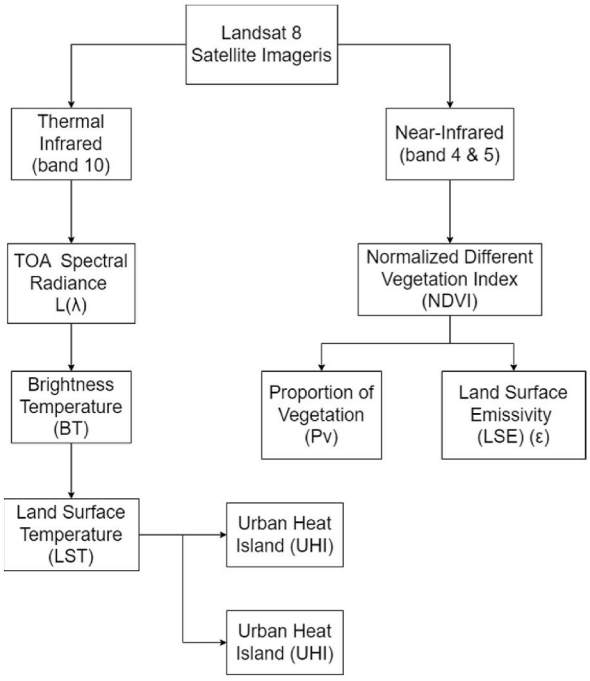

Fig. 4. Computation flow chart of the UHI and UTFVI mapping.

2.2. Satellite data

The Landsat-8 satellite's surface reflectance records were utilized. The three Landsat-8 bands used in this investigation were Band 4, Band 5, and Band 10. Only Band 4 can detect visible light thanks to its extremely short wavelengths; the rest of the bands operate in regions of the spectrum that are invisible to the human eye. The near-infrared, sometimes known as NIR, is what Band 5 measures. This region of the electromagnetic spectrum is particularly significant to the study of its ecology because healthy plants can reflect it; the water that makes up their leaves causes the wavelengths to be scattered back into the atmosphere. When supplemented with a measure such as the normalized difference vegetation index (NDVI), evaluating how green the plant is with the naked eye will not give users the most accurate judgment possible. Band 10 is located in the thermal infrared, also known as TIR, and can detect heat. This weather station does not measure the temperature of the air like other weather stations do; instead, it reports the temperature of the earth, which is typically significantly hotter. The satellite image and data were obtained from Survey [22]. The Landsat-8 imagery was obtained on the 24th of December 2021 and the November 16, 2013. Both dates were chosen since they are the oldest and most recent data available on the website for the KL area.

2.3. The computational mapping process

The computational flow chart for the entire process is shown in Fig. 4. The mapping of the UHI and the UTFVI is discussed in the subsections that follow. Each subsection was classified and reported on the computations and references utilized.

2.3.1. Urban heat island (UHI)

In general, the approaches for mapping the UHI may be broken down into three categories: those that use the LST as a proxy for SUHI, those that compare LST changes between urban and the surrounding areas (reference areas), and those that use statistical methods. Following the generation of the UHI data, they were separated into five distinct categories in Table 1. The UHI mapping approach utilized in this study is based on the previously mentioned reference urban point temperature i Pulau Tengah, Selangor.

As shown in Fig. 4 above, after extracting the landsat-8 images, the first step is to calculate the TOA (Top of Atmospheric), L(λ) spectral radiance using Eq. (1).

$$TOA\ (\mathrm{L}(\lambda)) = ML \times Q_{cal} + AL \tag{1}$$

TOA (L(λ)) stands for Total Spectral Radiance, ML stands for the band-specific Multiplicative Rescaling Factor, Qcal refers to the Band 10 of Landsat 8, and AL stands for the Band-Specific Additive Rescaling Factor. Opening the MTL file, which is stored as a Text Document (.txt), is the only way to obtain the values for ML, Qcal, and AL. AL can be found in the MTL file by searching for RADIANCE ADD BAND 10 = 0.10000, while ML can be found in the MTL file by searching for RADIANCE MULT BAND 10 = 3.3420E-04. Qcal may be obtained by selecting the Band 10 of the Landsat 8 image.

Following the stage of determining the TOA, the next step entails converting the spectral radiance to the brightness temperature (BT), as shown in Eq. (2) by making use of the thermal constants [23].

$$BT = \frac{K2}{ln\left[\left(\frac{K1}{L\lambda}\right) + 1\right]} - 273.15 \tag{2}$$

The Top of the Atmosphere Brightness Temperature is denoted by BT, Total Spectral Radiance is denoted by Lλ, K1 K2 and CONSTANT BAND 10 are the other variables. As was said earlier, open the MTL file document in order to discover the values. K1 can be discovered by finding the value of CONSTANT BAND 10, which is 774.8853, and K2 can be found by finding the value of CONSTANT BAND 10, which is 1321.0789. The TOA is the output from the step before it, and its output is the Lλ.

The following stage in the process is the Normalized Different Vegetation Index (NDVI) Method for Emissivity Correction based on Eq. (3). Since of this, the NDVI is extremely important because it must be used to calculate the proportion of vegetation (Pv), which is closely tied to the NDVI, as well as emissivity (ε), which is related to the Pv.

$$NDVI = \frac{NIR(band\ 5) - Red\ (band\ 4)}{nNIR(band\ 5) + Red\ (band\ 4)} \tag{3}$$

Solving for NDVI in Eq. (3), and substituting into Eq. (4), yields the proportion of vegetation P_v.

Table 1
UHI class.

Type	UHI value range	Class
1	<0.07	Very weak heat island
2	0.08–0.12	Weak heat island
3	0.13–0.17	Moderate heat island
4	0.18–0.20	Strong heat island
5	>0.21	Very strong heat island

$$P_v = \frac{NDVI - NDVI_{min}}{NDVI_{max} - NDVI_{min}}^2 \quad (4)$$

$NDVI_{min}$ refers to the previous result of NDVI minimum value while $NDVI_{max}$ refers the NDVI maximum value. Afterwards, the next step is to calculate the Land Surface Emissivity (LSE) (ε) using Eq. (5):

$$\in = 0.004 \times P_V + 0.986 \quad (5)$$

0.004 from MTL file and the value of 0.986 corresponds to a correction value of the equation.

The final step before calculating the UHI value was to compute the LST, which can be achieved using the following methods:

a) Brightness Temperature(BT)

Based on the previous BT value obtained from Eq. (2), the LST can be computed using Eq. (6):

$$LST = \frac{BT}{\left\{1 + \left[\left(\frac{\lambda BT}{\rho}\right) ln\, \varepsilon\right]\right\}} \quad (6)$$

BT is Top of Atmosphere Brightness Temperature, λ is the Emitted Radiance (λ is 10.895). ε is Land Surface Emissivity, $\boldsymbol{\rho} = 1.438 \times 10^{-2}$ m K, = 14,388 (ρ = h(c/σ), c is Boltzman constant (1.38×10^{-23} J/K), σ is velocity of light (2.998×10^{4} m/s) and h is Planck constant (6.626×10^{-34} J).

b) Radiation Transfer Equation (RTE)

The apparent radiance obtained by a sensor Bi(LST) from Landsat 8 images can be estimated below using Eq. (7), a simplified radiation transfer equation:

$$\mathrm{Bi(LST)} = \tau_i \left\lfloor \epsilon_i \mathrm{B_i(LST)} + (1 - \epsilon_i) \mathrm{I_i^{\downarrow}} \right\rfloor + \mathrm{I_i^{\uparrow}} \quad (7)$$

Where ϵi represents the land emission sensitivity, $\mathrm{I_i^{\uparrow}}$ and $\mathrm{I_i^{\downarrow}}$ represent the upwelling and downwelling radiance, respectively, τ_i represents the atmosphere transmissivity between the sensor and observed surface.

Subsequently, by applying the inverse of Planck's law on Eq. (7), the LST can also be computed, as shown in Eq. (8):

$$\mathrm{LST} = \frac{\mathrm{C1}}{\lambda_i \ln\left(\frac{\mathrm{C2}}{\lambda_i^5 \left(\mathrm{B_i(T_i)} - \mathrm{I_i^{\uparrow}} - \tau_i(1-\epsilon_i)\mathrm{I_i^{\downarrow}}\right)/\tau_i \epsilon_i} + 1\right)} \quad (8)$$

where λ_i is the effective band wavelength for band *i*, C1 is 14387.7 μm K, C2 is 1.19104 × 108 W·μm4·m−2·sr−1.

Lastly, the UHI value calculation can be obtained by Eq. (9):

$$UHI = \frac{LST_{urban} - LST_{rural}}{LST_{rural}} \quad (9)$$

2.3.2. Urban thermal field variance index (UTFVI)

UTFVI is a common measurement that assesses the presence of thermal comfort in the environment to determine the state of the environment and the condition of urban health. This is accomplished by using the temperature at which people feel most comfortable in their surroundings [24]. Eq. (10) serves as the foundation for its computation, and it is one of the indications that is utilized the vast majority of the time. Following the generation of the UTFVI data, they were separated into six distinct categories in Table 2 with the goals of enhancing the display and presenting more detailed environmental condition patterns around the city [25].

$$UTFVI = \frac{LST - LST_{mean}}{LST_{mean}} \quad (10)$$

Table 2
UTFVI class.

Type	UTFVI value range	Environmental Condition Category
1	<0.0	Very good
2	0.000–0.005	Good
3	0.005–0.010	Normal
4	0.010–0.015	Bad
5	0.015–0.020	Worse
6	>0.020	Worst

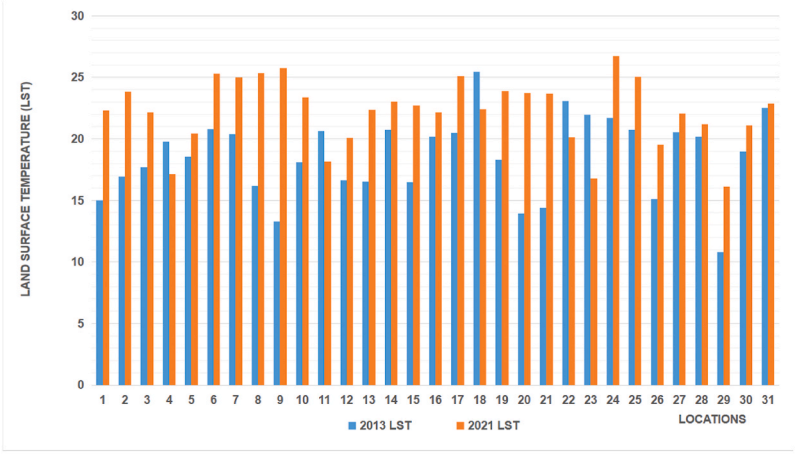

a) LST

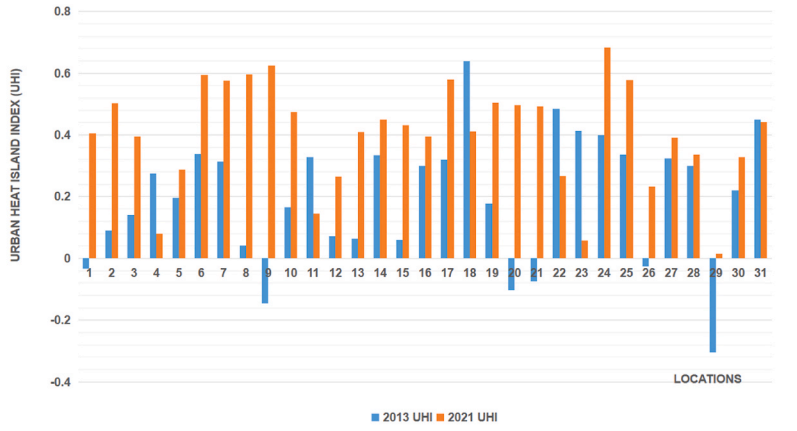

b) UHI

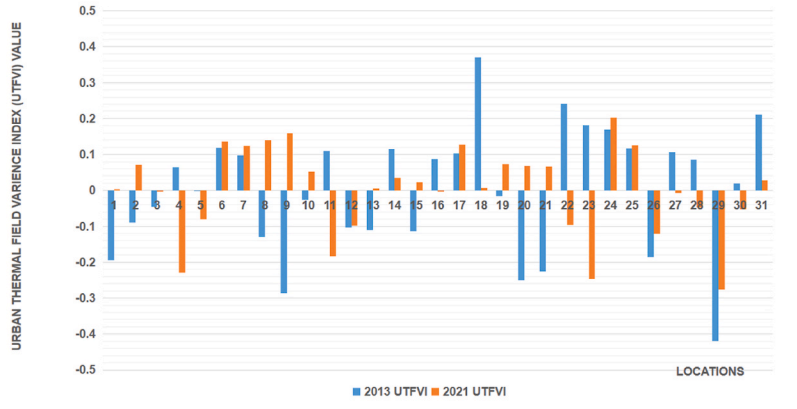

c) UTFVI

Fig. 5. The difference in the: a) LST, b) UHI, and c) UTFVI between 2013 and 2021.

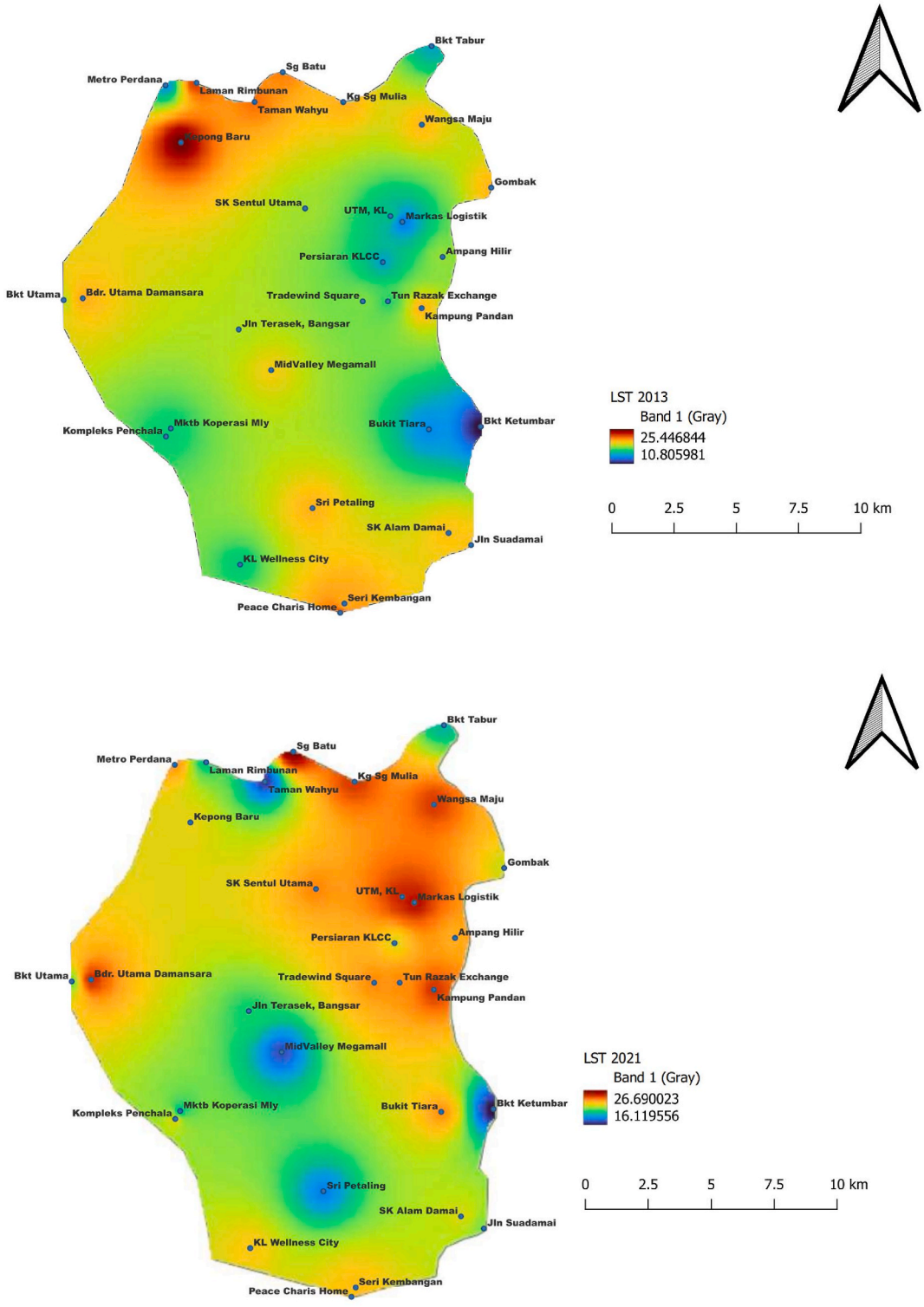

Fig. 6. LST in 2013 (top) and 2021 (bottom) (the chart labelled 1 from left to 31 towards right).

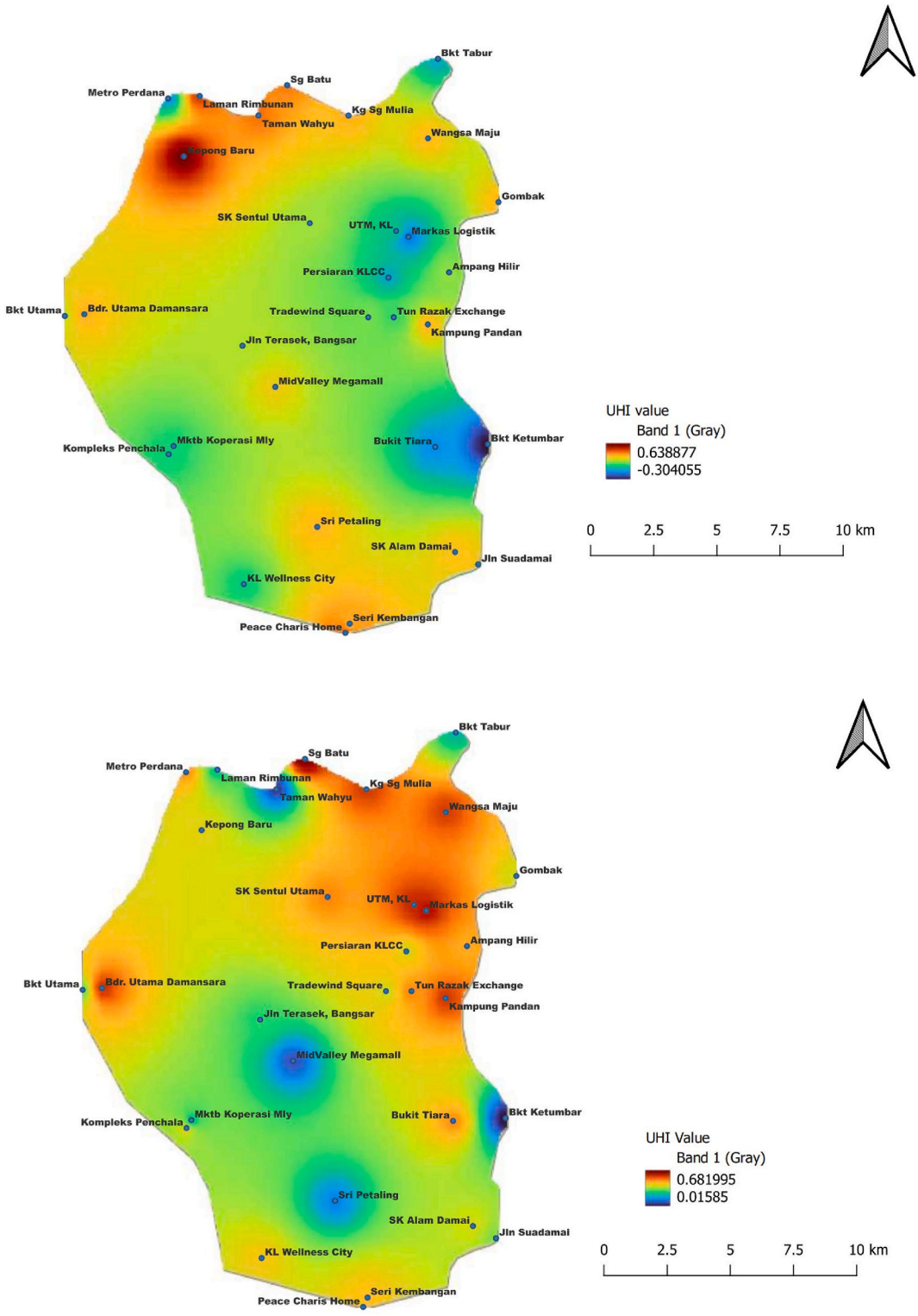

Fig. 7. UHI in 2013 (top) and 2021 (bottom) (the chart labelled 1 from left to 31 towards right).

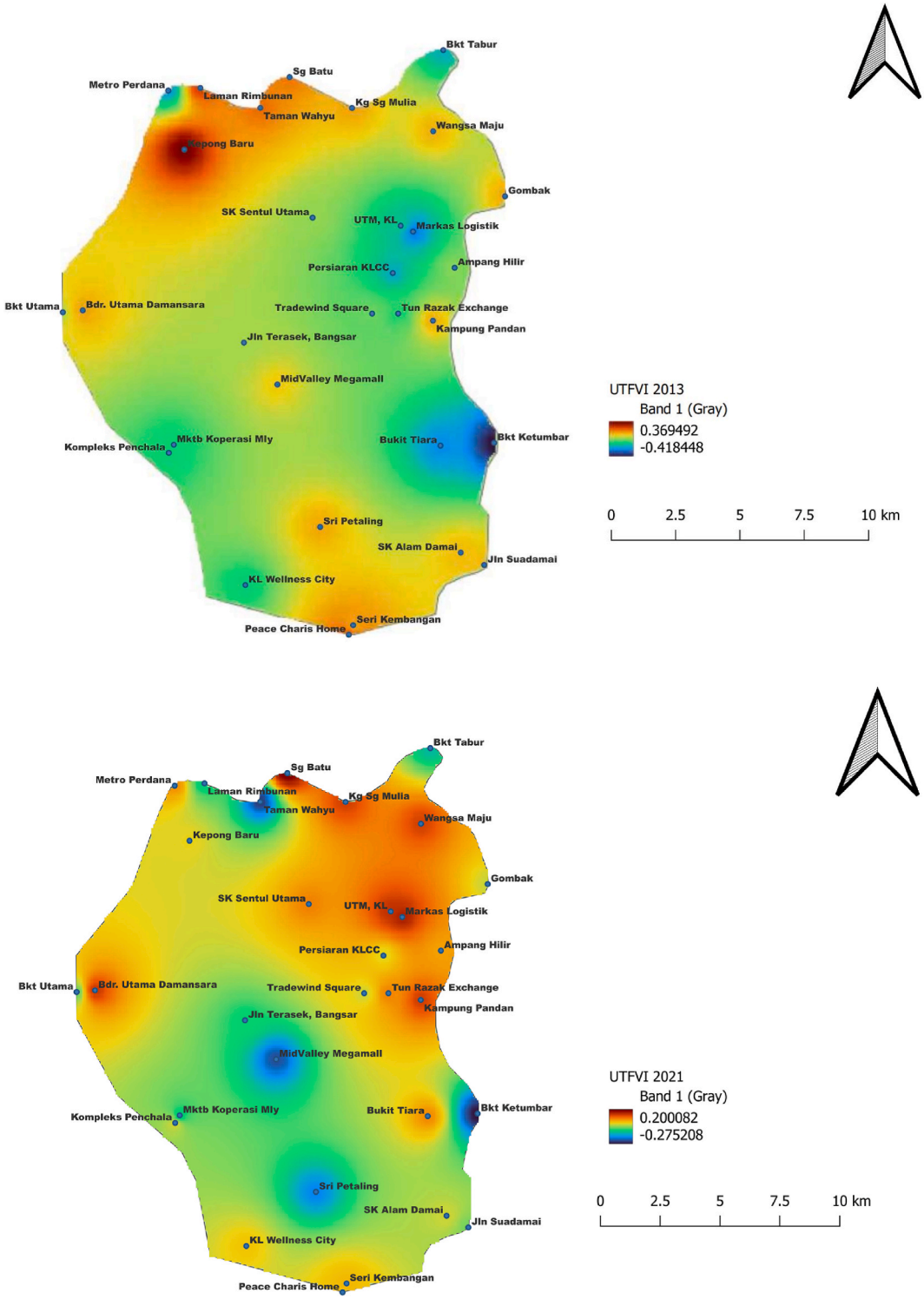

Fig. 8. UTFVI in 2013 (top) and 2021 (bottom) (the chart labelled 1 from left to 31 towards right).

3. Results and discussion

3.1. Masking and extracting map

As previously said, there are several methods of raster analysis, such as hill shadow, slope, data metrics grid, etc. However, in this research, the technique used was Grid (Inverse Distance to a Power) interpolation. The Inverse Distance to a Power gridding method is an example of an interpolator that uses weights to create an average. The output value of a cell generated with inverse distance weighting (IDW) is limited to the range of values used in the interpolation procedure. Because IDW is a weighted distance average, the average can never be more than or less than the greatest or lowest input. Interpolation using IDW takes significantly less time to process and is not affected by trends in data going in several directions. By specifying a higher power in IDW, more emphasis is placed on the points closer to each other, resulting in a more detailed surface.

After the raster data was interpolated, it was retrieved and clipped with the mask layer - in this case, the outline map of Kuala Lumpur created by making a Polygon shapefile of the map - to provide the appropriate mapping analysis. The generated maps were in the grey shades band, which was altered to a band of pseudo colors to generate the maps displayed.

3.2. LST, UHI and UTFVI tabulation and mapping

Following that, the bar charts (Fig. 5a–c) and the maps (Figs. 6–8) of LST, UHI, and UTFVI in 2013 and 2021 are generated. Table 3 below summarizes the location of the numbered point with their coordinates.

3.3. Variation of LST value over the year 2013 and 2021

Table 4 summarizes the computed LST values calculated using GIS software and the measured air temperature obtained from World Weather Online. To begin with, the temperature of the land surface relates to how heated the "surface" of the Earth would feel to a person who touched it. It may be compared to how warm a person's hand feels when it touches the Earth's surface. When a satellite looks down through the atmosphere, everything it sees is called the surface. The LST value obtained in 2021 was, on average higher than in 2013, with a reading of 22.2401° Celsius. The maximum LST in 2021 was 26.729° Celsius, whereas the highest in 2013 was 25.448° Celsius. A comparison was performed to establish the differences between LST and observed air temperature. A negative

Table 3
Coordinates of point location.

No.	Location	Latitude	Longitude
1	Persiaran KLCC	3.15665	101.71826
2	Tun razak exchange	3.1425	101.72012
3	Tradewind Square	3.15185	101.71102
4	Mid valey Megamall	3.11768	101.67793
5	Jalan Terasek, Bangsar	3.13236	101.66621
6	Bandara Utama Damansara Utama	3.14361	101.60986
7	Jalan a8/278, Wangsa Maju	3.20622	101.73237
8	Universiti Teknologi Malaysia, KL	3.17324	101.721
9	Markas Logistik Tentera Barat, Dato Keramat	3.17115	101.72534
10	Ampang Hilir	3.15852	101.73987
11	Sri Petaling	3.06788	101.69288
12	Maktab Koperasi Malaysia, PJ	3.09376	101.641684
13	Kompleks Penchala, PJ	3.09376	101.63995
14	Jalan Utama, Seri Kembangan	3.03347	101.70441
15	KL wellness city	3.04754	101.66671
16	Sekolah Kebangsaan Alam Damai	3.05891	101.742006
17	Kampung Pandan	3.14	101.7323
18	Jalan Pelandok, Kepong Baru	3.19982	101.64535
19	Sekolah Kebangsaan Sentul Utama	3.17602	101.69021
20	Bukit Tiara, Cheras	3.09631	101.73492
21	Metro Perdana	3.22045	101.63977
22	Laman Rimbunan	3.22134	101.65098
23	Taman Wahyu	3.2144	101.67196
24	Sungai Batu	3.22518	101.68215
25	Kampung Sungai Mulia	3.21435	101.704004
26	Bukit Tabur	3.2346	101.7359
27	Gombak	3.18352	101.75746
28	Jalan Suadamai	3.05455	101.7502
29	Bukit Ketumbar	3.09729	101.75366
30	Bukit Utama	3.14296	101.60293
31	Peace Charis Home	3.03013	101.702888

Table 4
Summary of LST and measured air temperature for the year 2013 and 2021.

Features	2013			2021		
	LST	Measured	Difference	LST	Measured	Difference
Min	10.800	22.000	−11.200	16.113	22.000	−5.887
Max	25.448	31.000	−5.552	26.729	32.000	−5.271
Mean	18.581	26.125	−7.544	22.240	25.875	−3.635
Std Dev	3.238	3.182	0.056	2.705	3.563	−0.858

difference implies a higher LST estimation than the recorded temperature, while a positive difference suggests a lower LST assessment than the recorded value. All LST datasets show the highest disparity in 2013, with differences in the minimum and maximum temperatures of 11.2 °C and 5.552 °C, respectively. The difference between estimated LST values and measured air temperature values can be attributed to the effects of surface roughness on surface temperature and atmospheric impurities that can obstruct the smooth passage of radiant energy [26]. Due to the discrepancies, it is necessary to compute the link between the estimated LST values and the measured surface temperature values, which might be accomplished by statistical regression analysis. The mean, maximum, and minimum temperature values for the date of collection mentioned above were used in the analysis. Based on the results, an R2 of 0.9929 in 2013 and 0.6668 in 2021, as shown in Fig. 9aandb, revealed a substantial association between LST and observed air

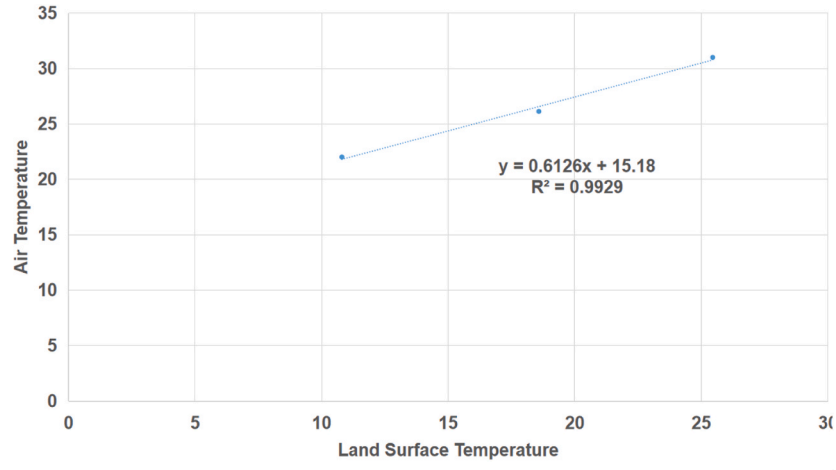

a) 2013

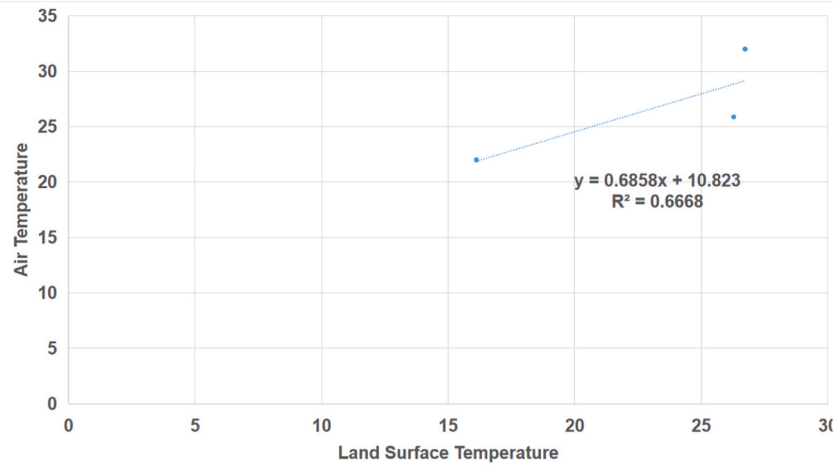

b) 2021

Fig. 9. Statistical analysis between LST and measured air temperature in a) 2013 and b) 2021.

temperature despite the underestimated LST values.

The temperature of the land's surface is a critical reference index used in assessing the condition of the land's environment. It affects the area's material and energy cycles, the ecological system's stability, the development of people, and human existence, as well as other factors. One of the reason behind the increase in the LST value in KL is, as previously mentioned above, the constant and consistent construction of buildings and deforestation. According to Fig. 6, in the upper right section of the map in 2013, the region looked to be more blue and green (indicating lower LST), but by 2021, the hue switched to appear to be more red and orange (meaning higher LST). It is due to the building that has occurred in the intervening years. An ANOVA analysis was also conducted to investigate the statistically significant differences between the temperature variations throughout the research period. The results of the two-way ANOVA with repeated measures were tabulated in Table 5, revealing evidence of a statistically significant interaction between group and time ($p = 9.86E\text{-}06$), indicating that Kuala Lumpur had undergone a statistically noteworthy rise in temperature from the years 2013–2021.

The Tun Razak Exchange, originally known as the Kuala Lumpur International Financial District or KLIFD, now undergoing finishing development in the middle of Kuala Lumpur, is one of the more notable projects in the city. The goal is to act as a strategic enabler for the Malaysian government's Economic Transformation Programme (ETP). This project began in 2017 and is estimated to take 15 years to complete, increasing the number of LSTs. It is evident in the mapping in Fig. 6, where the color changes from blue and green to red and orange in the specific area. To be more exact, the LST value of the region revealed that where the temperature was 16.919° Celsius in 2013, it had grown to 23.847° Celsius in 2021. As construction is currently taking place, there will be a significant increase in the number of machines used to transport the materials. This results in a considerable rise in both traffic and air pollution, which not only contribute to the emission of carbon dioxide but also inadvertently bring about an increase in LST. Higher LST causes a decline in human thermal comfort in urban settings, which has consequences for both the urban environment and nature. The temperature rises at the land's surface have been linked to severe adverse effects on human health.

3.4. Relationships between UHI and UTFVI indices with urban population (or density)

As urban population densities grow and consequentially natural land areas slowly disappearing, heat islands will become increasingly common. Urbanization occurs largely as a result of migration from rural to urban areas, which increases the urban population and the size of urban areas. According to several researches, KL is an expanding city, implying that energy consumption and pollution are on the rise. Sprawling urban growth may worsen thermal conditions, adding to the UHI and UTFVI impact. Simply put, an urban heat island (UHI) is a phenomenon that arises when the average temperature in a city is noticeably higher than in the neighboring rural regions. The ability of surfaces in urban and less-developed rural areas to absorb and retain heat is a fundamental contributor to the large temperature discrepancy between these two habitats. To provide a more accurate description of the Surface Urban Heat Island (SUHI) effect, the UTFVI has become an increasingly used indicator [24]. Comparing different assessment metrics, UHI, and UTFVI revealed structural resemblance. Table 6 summarizes the computed UHI and UTFVI values calculated using GIS software.

The positive relationships between UHI and industry expansion reveal that areas with more industrial development and economic growth tend to experience lower temperatures in the vicinity. The results of UHI and UTFVI patterns of all areas show that Pulau Tengah was cooler than others, exhibiting a cool island phenomenon. Pulau Tengah is a tiny island near Pulau Ketam, populated by mangrove woods. Due to this, the LST was typically low and comparable to the nearby urban area (15.527° Celsius in 2013 and 15.868° in 2021). Compared to the previous similar work in 2013, the present study in 2021 demonstrates a significant variation in terms of cool and heat island location and quantity, along with the intensity of the city's UHI. From six cool islands in 2013, the number has significantly decreased to zero. In other words, throughout the period from 2013 to 2021, those cool islands experienced urbanization, causing increasing in temperature, and thus ending up with higher UHI values. A general trend can be observed from Fig. 7, which is a shift from the west to the east part of KL. Despite having an increase in the heat islands inside the city, some locations, as indicated in Table 7, experienced the opposite effect. Some studies demonstrated that the population density in the KL city center area is decreasing, despite showing a significant strong positive relationship between the intensity of the urban heat island of the city of KL with the population density. These locations, despite having ranked high in 2013, due to urbanization focusing on the northern east part of KL, the population remained unaffected. Also, as observed, the heat islands are mostly concentrated inside the city center; however, a recent study shows that the majority of heat islands are gradually turning into cool islands. Previously, the highest UHI value or center of the city's UHI was located within the city center; however, the study shows that the value position has shifted. It was located in the (Taman Wahyu and Laman Rimbunan) area, but according to research, it is currently located at Sungai Batu.

Overall, compared to the average UHI value in 2013, which was 0.1967, the average UHI value for the year 2021 was 0.40157, which was higher. The findings are also compatible with those of Wang, Aktas [5], who indicated that the UHI is growing at a rate that might endure for decades. Ramakreshnan, Aghamohammadi [27] followed on to undertake research to determine the underlying

Table 5
The Analysis of Variance (ANOVA) results on the temperature difference in year 2013 and 2021.

Source of variation	SS	df	MS	F	p-value
between group	207.505	1.00	207.51	23.32	9.86E-06
within group	533.972	60.00	8.90		
total	741.478	61			

Table 6
Summary of UHI and UTFVI for the year 2013 and 2021.

Features	2013		2021	
	UHI	UTFVI	UHI	UTFVI
Min	−0.3044	−0.4188	−0.3044	−0.4188
Max	0.63895	0.36955	0.63895	0.36955
Mean	0.1967	0	0.1967	0
Std Dev	0.20852	0.17425	0.20852	0.17425

Table 7
Locations where UHI was reduced.

Locations	Changes in UHI
Mid valey Megamall	−0.194
Sri Petaling	−0.183
Laman Rimbunan	−0.227
Taman Wahyu	−0.217

causes of the growth in UHI in Kuala Lumpur. They demonstrated that land use changes, built-up regions, and, in particular, a decline in green space are the major causes of the growth. All of these studies concur that the rising urban heating problem in Kuala Lumpur results with urban expansion. We are often reminded that an urban heat island arises when the average temperature in a city is much higher than in nearby rural regions.

The Sungai Batu point location, located in the center of the top of Fig. 1, yielded the highest reading of 0.39847 and 0.68446 in the years 2013 and 2021. The region is located in the Kawasan Perindustrian Spring Crest and is also known as the industrial area of Batu Cave. The phrase "industrial area" refers to where the main activity is the production, accumulation, processing, or other treatment of raw materials, partially produced goods, or finished goods for packaging and distribution to either wholesale or retail markets. One example would be the production of raw materials for other types of raw materials. This location, for example, is home to various construction enterprises, including hardware and motorbike stores, among many others. Burning fossil fuels for energy production, industrial processes, and transportation is the primary focus of the activities and operations that take place in the region. These are some of the most significant factors that contributed to the high value of the UHI. Other economic pursuits, such as manufacturing, also contributed significantly. It is because these activities are responsible for the emission of significant quantities of greenhouse gases, such as carbon dioxide, into the atmosphere. Compared to the emission in rural areas, the amount emitted in this urban area appear to be significantly larger, thus resulting in a high UHI value.

Fig. 8 depicts the mapping and analysis of the UHI for 2013 and 2021. The Bandar Damansara Utama point position on the left side of the map shows a rise in the UHI value, indicating a positive correlation between UHI and population, as evidenced by the fact that in 2013, the region had a population of at least 11,539 people. However, in 2021, the population was expected to reach at least 19,205 people (based on Department of Statistics web data). The element that contributes the highest to the high population density is people moving from more rural areas to urban centers in search of employment opportunities. As more people start to live in a region, the population density increases, and with it comes the inevitable problem of increased congestion [28]. It includes issues such as overcrowded roads and transportation congestion, which makes it more difficult for people to travel by public transportation, which leads to more people purchasing cars, which in turn leads to additional issues such as traffic jams and pollution.

The lowest UHI value from the 31-point locations was at the Bukit Ketumbar point location. The reading from 2013 was −0.3044 and 0.0154 in 2021. The low value is because the data were gathered in a woodland region. Increasing the amount of vegetation in a place is a simple and effective way to reduce urban heat islands since trees and other plants contribute to a colder atmosphere. By casting their shadows on the ground and allowing water to evaporate into the atmosphere, trees and other forms of vegetation can bring surface and air temperatures down. This reasoning is also consistent with the findings of Harun, Reda [10], who discovered that land cover plays a significant role in temperature fluctuations within cities. Regardless of other environmental factors, vegetation regions are somewhat cooler than other locations. The higher thermal conductivity increases the amount of heat absorbed, slowing the pace of cooling and hence causing the UHI to be high. Thus, it is best to believe that the presence of greenery in the urban area can help to bring down the UHI value.

4. Conclusions

The primary motivating reason that makes this study essential and required is the progression of climate change and the accompanying temperature rise. Thus the partial reasons that contribute to this temperature rise, apart from the well-known industrialization that had taken place in the intervening years, within the climate change phenomenon have to be identified. Data from the end of the year 2013, as well as data from 2021, were included in the mapping analysis. Besides, time-series Landsat-8 satellite pictures were utilized to explore the temporal shifts in LST, UHI, and UTFVI across Kuala Lumpur. The maps produced to depict LST, UHI, and UTFVI in Kuala Lumpur between 2013 and 2021 are the essential takeaways from this research. This study also provided data and analytical comparisons for the two years.

It is essential to have a good understanding of the urban heat island effect in Kuala Lumpur if one is to design methods to reduce or to mitigate the harmful effects of the UHI. It can entail implementing techniques to reduce the amount of heat-absorbing materials used throughout the city, such as installing green walls and roofs. Modeling the urban heat island effect in Kuala Lumpur helps advise city planners and decision-makers on the most effective methods for controlling the temperature and preventing the adverse effects of the urban heat island effect on the local environment and the local population. It can help to develop a more live-able and a sustainable city for everyone.

Author contribution statement

Nasrin Adlin Syahirah Binti Kasniza Jumari: Conceived and designed the experiments; Performed the experiments; Analyzed and interpreted the data; Wrote the paper.

Ali Najah Ahmed; Chai Hoon Koo; Kai Lun Chong; Mohsen Sherif; Ahmed Elshafie: Conceived and designed the experiments; Analyzed and interpreted the data; Wrote the paper.

Yuk Feng Huang: Conceived and designed the experiments; Analyzed and interpreted the data; Contributed reagents, materials, analysis tools or data; Wrote the paper.

Jing Lin Ng: Conceived and designed the experiments; Analyzed and interpreted the data.

Data availability

Data will be made available on request.

Additional information

No additional information is available for this paper.

Declaration of competing interest

The authors declare that they have no known competing financial interests or personal relationships that could have appeared to influence the work reported in this paper.

Acknowledgements

This study was funded by Universiti Tunku Abdul Rahman (UTAR), Malaysia, via Project Research Assistantship (Project Number: UTARRPS 6251/H03). The authors would also like to acknowledge EarthExplorer as the data provider for the Landsat-8 images data.

References

[1] W. Zhang, et al., Improved combined system and application to precipitation forecasting model, Alex. Eng. J. 61 (12) (2022) 12739–12757.
[2] R. Lindsey, L. Dahlman, Clim. Change: Global temperature (2020). Available online: climate. gov (accessed on 22 March 2021.
[3] F.T. Najah, S.F.K. Abdullah, T.A. Abdulkareem, Urban land use changes: effect of green urban spaces transformation on urban heat islands in baghdad, Alex. Eng. J. 66 (2023) 555–571.
[4] N. Li, S. Miao, Y. Wang, The future urban growth under policies and its ecological effect in the Jing-Jin-Ji area, China, Heliyon 7 (4) (2021), e06786.
[5] K. Wang, et al., Urban heat island modelling of a tropical city: case of Kuala Lumpur, Geoscience Letters 6 (1) (2019) 1–11.
[6] G.N. Yuan, et al., A Review on Urban Agriculture: Technology, Socio-Economy, and Policy, Heliyon, 2022, e11583.
[7] H.I. Effect, Heat island effect, Available from: https://www.epa.gov/heatislands, 2022.
[8] R. Bala, R. Prasad, V.P. Yadav, A comparative analysis of day and night land surface temperature in two semi-arid cities using satellite images sampled in different seasons, Adv. Space Res. 66 (2) (2020) 412–425.
[9] R. Bala, R. Prasad, V.P. Yadav, Quantification of urban heat intensity with land use/land cover changes using Landsat satellite data over urban landscapes, Theor. Appl. Climatol. 145 (2021) 1–12.
[10] Z. Harun, et al., Urban heat island in the modern tropical Kuala Lumpur: comparative weight of the different parameters, Alex. Eng. J. 59 (6) (2020) 4475–4489.
[11] N.D.A. Halim, et al., The long-term assessment of air quality on an island in Malaysia, Heliyon 4 (12) (2018), e01054.
[12] M. Lum, The Effects of Climate Change in Malaysia, Available from:, 2022 https://www.thestar.com.my/lifestyle/health/the-doctor-says/2022/07/05/the-effects-of-climate-change-in-malaysia.
[13] K.I. Morris, et al., Numerical study on the urbanisation of Putrajaya and its interaction with the local climate, over a decade, Urban Clim. 16 (2016) 1–24.
[14] A. Mahdavi, K. Kiesel, M. Vuckovic, Methodologies for UHI Analysis. Counteracting Urban Heat Island Effects in a Global Climate Change Scenario, 2016, p. 71.
[15] M.P. Acosta, et al., How to bring UHI to the urban planning table? A data-driven modeling approach, Sustain. Cities Soc. 71 (2021), 102948.
[16] G. Mutani, V. Todeschi, K. Matsuo, Urban heat island mitigation: a GIS-based model for Hiroshima, Instrumentation, Mesures, Métrologies 18 (4) (2019).
[17] S. Jain, et al., Urban heat island intensity and its mitigation strategies in the fast-growing urban area, Journal of Urban Management 9 (1) (2020) 54–66.
[18] B. Markham, Landsat Science - Landsat 8, Available from:, 2013 https://landsat.gsfc.nasa.gov/landsat-data-continuity-mission/.
[19] R. Bala, R. Prasad, V.P. Yadav, Disaggregation of modis land surface temperature in urban areas using improved thermal sharpening techniques, Adv. Space Res. 64 (3) (2019) 591–602.
[20] R. Analysis, Raster Analysis in QGIS, Available from:, 2022 https://gisrsstudy.com/qgis-raster-analysis/.
[21] A.K. Jebur, Uses and applications of geographic information systems, Saudi J. Civ. Eng 5 (2021) 18–25.
[22] U.S.G. Survey, Available from: EarthExplorer (2015) http://earthexplorer.usgs.gov/.
[23] U. Avdan, G. Jovanovska, Algorithm for automated mapping of land surface temperature using LANDSAT 8 satellite data, J. Sens. (2016) 2016.
[24] A.-A. Kafy, et al., Prediction of seasonal urban thermal field variance index using machine learning algorithms in Cumilla, Bangladesh, Sustain. Cities Soc. 64 (2021), 102542.

[25] S. Guha, et al., Analytical study of land surface temperature with NDVI and NDBI using Landsat 8 OLI and TIRS data in Florence and Naples city, Italy. European Journal of Remote Sensing 51 (1) (2018) 667–678.
[26] A. Ngie, et al., An estimation of land surface temperatures from landsat ETM+ images for Durban, South Africa, Rwanda Journal (2016) 1.
[27] L. Ramakreshnan, et al., A Critical Review of Urban Heat Island Phenomenon in the Context of Greater Kuala Lumpur, Malaysia vol. 39, Sustainable Cities and Society, 2018, pp. 99–113.
[28] I.S. Elsayed, Effects of Population Density and Land Management on the Intensity of Urban Heat Islands: A Case Study on the City of Kuala Lumpur, Malaysia. Application of Geographic Information Systems, 2012, pp. 267–283.